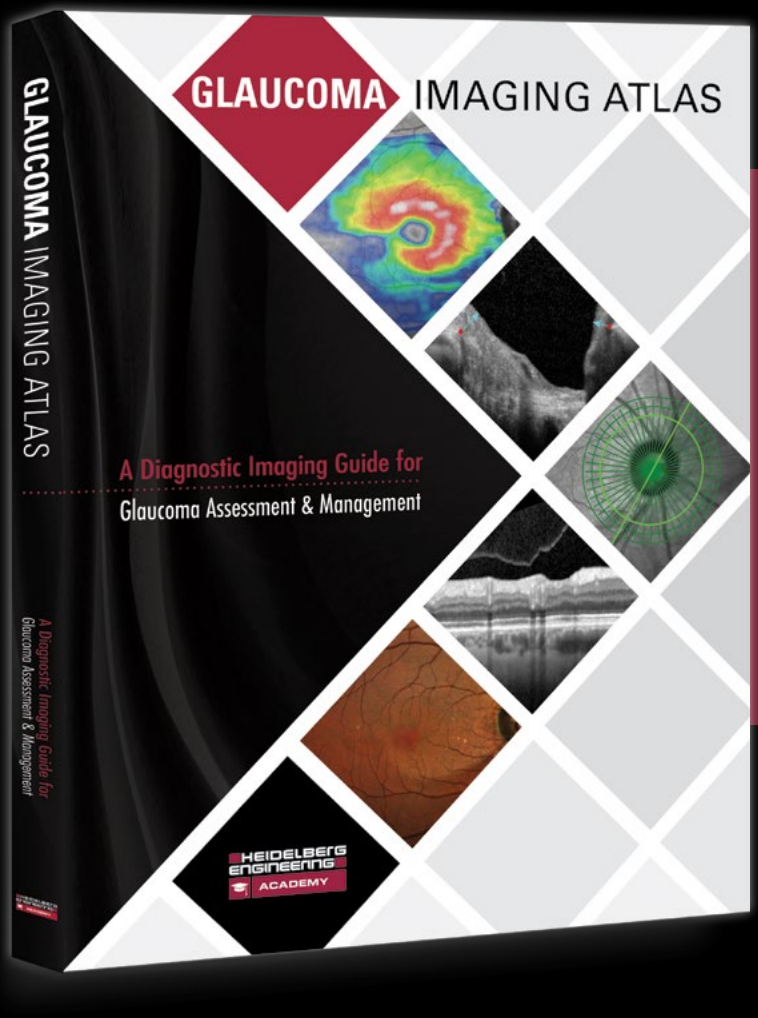

GLAUCOMA IMAGING ATLAS

PREVIEW

With clinical case studies from:

- Murray Fingeret, OD
- Min Hee Suh, MD
- Donald C. Hood, PhD, and Robert Ritch, MD

HEIDELBERG ENGINEERING
ACADEMY

Introduction

Glaucoma is a leading cause of irreversible vision loss worldwide. Because it may be asymptomatic until a relatively late stage, diagnosis is frequently delayed. A general understanding of the disease pathophysiology, diagnosis, and treatment may assist primary care physicians in referring high-risk patients for a comprehensive ophthalmology examination and in participating more actively in the care of patients affected by this condition. Patients with primary open-angle glaucoma are not necessarily aware of the associated vision loss, as the disease usually progresses asymptomatically until advanced stages. Thus, open-angle glaucoma is generally detected incidentally during a comprehensive ophthalmic examination. By the time vision loss symptoms manifest, patients have already suffered substantial and irreversible neural damage. Vision loss results in reduced quality of life and a diminished ability to perform daily activities, such as driving. Therefore, early intervention is essential to slow the progression of the disease.

A Diagnostic Puzzle

There is no single perfect reference standard for the diagnosis of glaucoma, and accurate diagnosis can be challenging even by trained ophthalmic clinicians. Modern imaging methods such as spectral-domain optical coherence tomography (SD-OCT) enable clinicians to view the anatomical details of the macula, circumpapillary retinal nerve fiber layer (cRNFL), and optic nerve head in greater detail than ever before. The Heidelberg Engineering SPECTRALIS® SD-OCT Glaucoma Module Premium Edition (GMPE) offers unique OCT scan patterns based on the anatomy of each individual eye, allowing accurate and precise measurement of the ocular structures that are susceptible to glaucomatous damage. Infrared and MultiColor confocal scanning laser ophthalmoscope images complement the SD-OCT scans, offering value beyond fundus photography. Taken together, these powerful tools can help improve glaucoma care and management.

A Glaucoma Solution

The following case series is a subset from a more comprehensive SD-OCT glaucoma imaging atlas. The atlas aims to offer exemplary cases where SD-OCT imaging, combined with visual field testing, enhances the clinical diagnosis and management of glaucomatous optic neuropathy. More specifically, the cases focus on the robust software features used to derive the diagnostic parameters and why, in some instances, it is important to corroborate the SD-OCT results by carefully reviewing the associated B-scans.

Case Presentation 1: Confirmation of Early Glaucoma Establishes Baseline for Tracking Progression, Min Hee Suh, MD

A 51-year-old female patient presented with bilateral primary open-angle glaucoma (POAG). This case focuses on the left eye (OS) of this patient. She does not have a family history of glaucoma and has not undergone any ocular surgical procedures. Untreated, her intraocular pressure (IOP) was 39 mmHg OS with a central corneal thickness of 561 µm. After administration of topical hypotensive medications, her IOP was reduced to 10 mmHg. Fundus photographs show a focal temporal superior retinal nerve fiber layer (RNFL) defect and diffuse RNFL loss inferiorly (Fig. 1).

Standard Automated Perimetry (SAP) was performed on the Humphrey Field Analyzer (HFA) using the Swedish Interactive Thresholding Algorithm Standard (SITA-Standard) with the 30-2 test pattern. While the mean deviation (MD) results are "Within Normal Limits," the pattern standard deviation (PSD) and Glaucoma Hemifield Test (GHT) results are indicative of early loss of sensitivity (Fig. 2; MD = -0.51 dB; PSD = 2.16 dB, P < 10%; GHT = Borderline).

OS

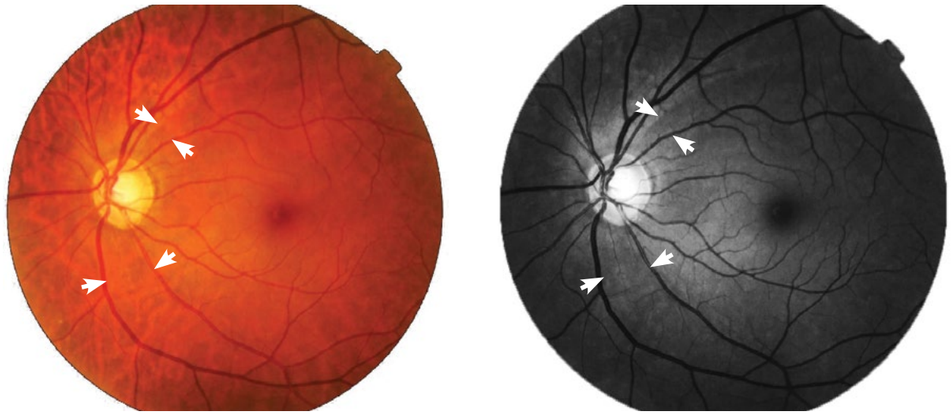

Figure 1. Fundus photographs show optic disc cupping and RNFL wedge defects superior and inferior to the optic nerve (white arrows).

OS

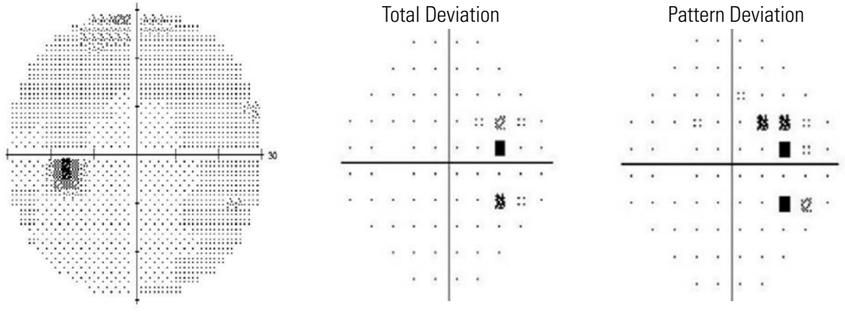

Figure 2. SAP results from the HFA using the SITA-Standard and 30-2 test pattern show signs of sensitivity loss in the inferior and superior hemifields. While the MD result is "Within Normal Limits" (MD = -0.51 dB), the PSD and GHT results are "Borderline" (PSD = 2.16 dB, P < 10%).

Diagnostic Imaging

The patient was imaged with the SPECTRALIS Glaucoma Module Premium Edition (GMPE) scans of the circumpapillary RNFL and the optic nerve head. The extensive inferior RNFL wedge defect is flagged as "Outside Normal Limits" on the 3.5 mm RNFL scan TSNIT profile results and on the 6-sector Garway-Heath analysis (Fig. 3). Although the temporal superior (TS) RNFL wedge defect is not flagged as abnormal on the 6-sector Garway-Heath analysis, the TS sector results are within the 9th percentile as compared with the reference database (RDB). Close examination of the 3.5 mm RNFL B-scan and TSNIT profile confirm this focal TS RNFL wedge defect. The 4.1 mm and 4.7 mm RNFL B-scans and the associated results further corroborate these findings. The Bruch's Membrane Opening - Minimum Rim Width (BMO-MRW) analysis indicates superior and inferior neuroretinal rim thinning (Fig. 4).

OS

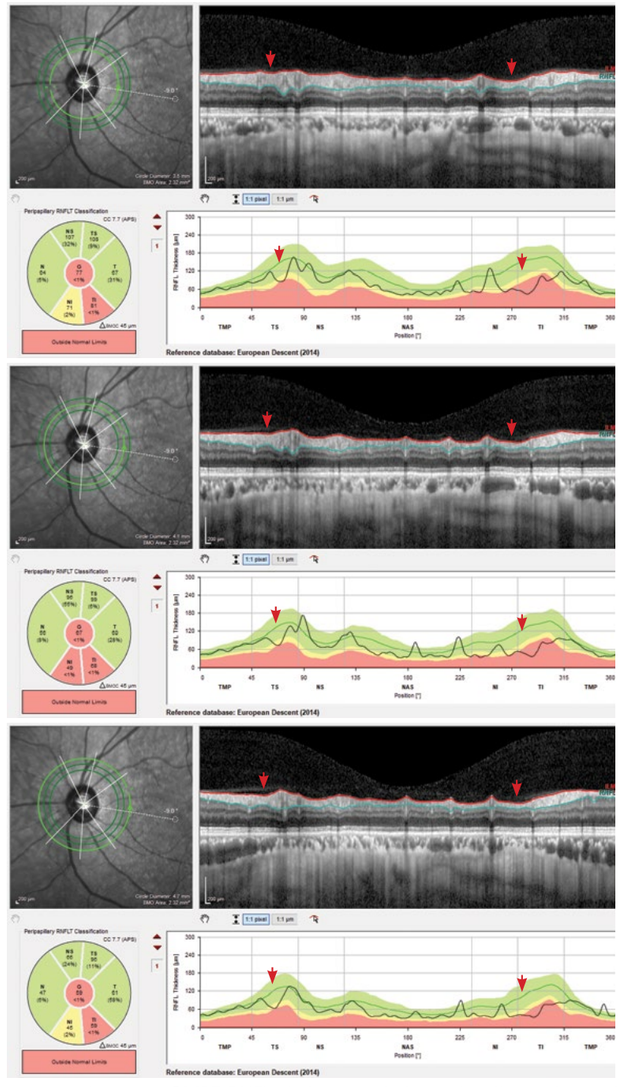

Figure 3. The 3.5 mm, 4.1 mm, and 4.7 mm GMPE RNFL circle scans help to visualize and quantify the inferior and superior wedge defects seen on the ophthalmic examination and on fundus photography. The TS RNFL wedge defect is confirmed on the B-scans and TSNIT profiles of each circle scan.

OS

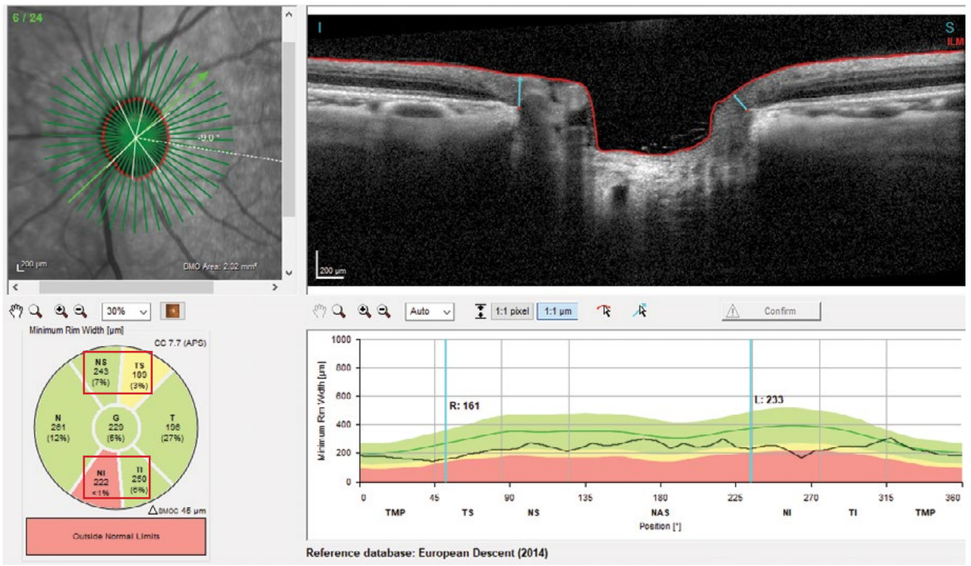

Figure 4. The BMO-MRW results indicate superior and inferior neuroretinal rim thinning.

Conclusion

This patient presented with a diagnosis of POAG in both eyes. While the SAP 30-2 results OS are indicative of potential early VF loss, the ophthalmic examination and fundus photography show clear signs of inferior RNFL loss and a focal TS RNFL wedge defect. The SPECTRALIS GMPE scan results confirm and quantify the extent of structural damage, especially in the inferior region. While the focal TS wedge defect is difficult to appreciate on sector classifications, closer inspection of the B-scans and the TSNIT profile confirm these defects. The BMO-MRW measurements indicate superior and inferior neuroretinal rim thinning, confirming the TS wedge defect results and indicating potential glaucomatous progression in this region. The extent of structural damage as measured by the RNFL and BMO-MRW parameters are strong indicators for the need to monitor this patient closely moving forward, especially since this damage has not yet fully manifested itself functionally.

Min Hee Suh, MD

Assistant Professor, Department of Ophthalmology, Inje University Haeundae Paik Hospital, Busan, Korea

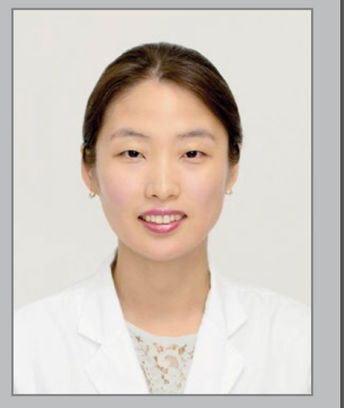

Dr. Min Hee Suh completed a residency in ophthalmology and a fellowship in glaucoma at Seoul National University Hospital in Seoul, Korea. She was an instructor in the department of ophthalmology at Myung-ji Hospital and a visiting scholar at the ophthalmology department of the University of California San Diego prior to joining the faculty at Inje University Haeundae Paik Hospital in 2011. Dr. Suh has published numerous scientific papers, and she received an award for outstanding scientific paper from the Korean Society of Ophthalmology in 2010. She is a member of the Korean Ophthalmological Society, Korean Glaucoma Society, and World Glaucoma Association.

Case Presentation 2: Focal Structural Damage with Corresponding Functional Loss, Murray Fingeret, OD

A 60-year-old male was recently diagnosed with primary open-angle glaucoma (POAG). He does not have a family history of glaucoma, and he presented with intraocular pressures (IOP) of 16 mmHg in the right eye (OD) and 17 mmHg in the left eye (OS). Corneal pachymetry measurements were 576 µm in each eye. This case focuses on the right eye of this patient. A superior retinal nerve fiber layer (RNFL) wedge defect can be seen on the SPECTRALIS MultiColor fundus image (Fig. 1, OD).

Standard Automated Perimetry (SAP) was performed with the Humphrey Field Analyzer (HFA) using the Swedish Interactive Thresholding Algorithm Standard (SITA-Standard) and 24-2 test pattern (Fig. 2). The HFA mean deviation (MD) and pattern standard deviation (PSD) results were both "Outside Normal Limits." The observed visual field (VF) defects correspond in location to the RNFL wedge defect identified on MultiColor imaging. The field results were confirmed with fundus automated perimetry (FAP) using the CenterVue Compass perimeter using the Zippy Estimation by Sequential Testing (ZEST) strategy and the 24-2 test pattern. The MD and PSD for this test were -2.29 dB and 3.67 dB, respectively (Fig. 3).

OD

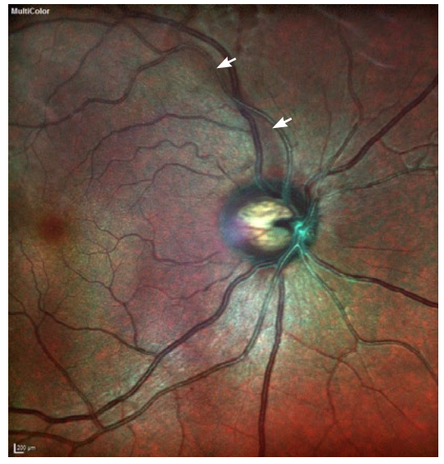

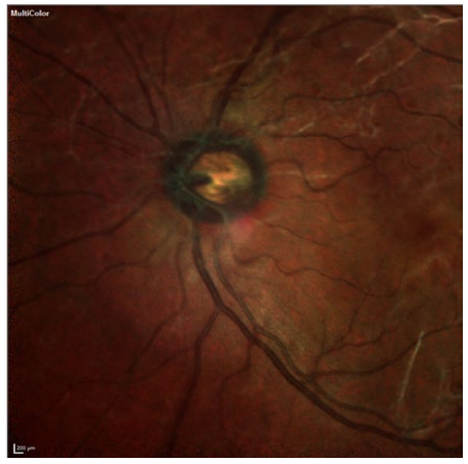

OS

Figure 1. The SPECTRALIS MultiColor image shows a wedge defect in the superior retina of the right eye (OD, white arrows). The left eye (OS) appears normal, though the MultiColor image is of poor quality due to media opacity.

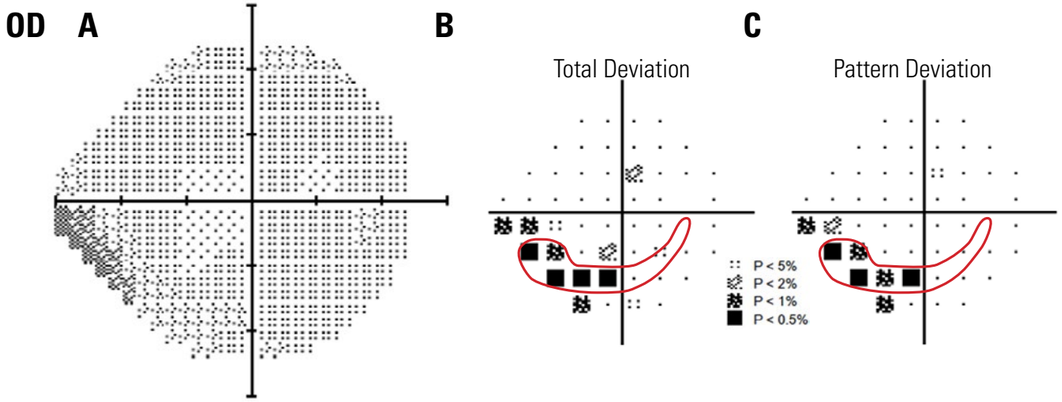

Figure 2. (A) Greyscale representation of the HFA VF shows abnormal test locations in the inferior hemisphere. The Total Deviation (B) and Pattern Deviation (C) maps show loss of sensitivity in the inferior hemisphere (red outline), corresponding to the wedge defect in the superior retina. The MD and PSD for this test were -2.56 dB, P < 5% and 2.88 dB, P < 2%, respectively.

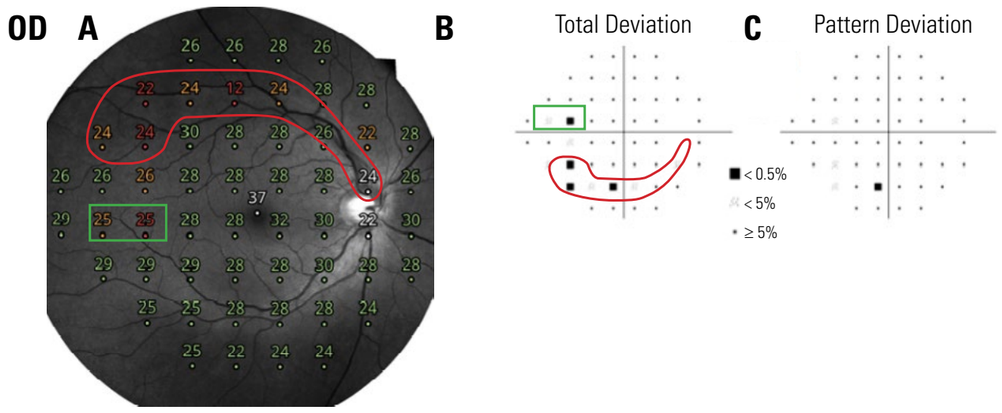

Figure 3. (A) The sensitivity measurements (in dB) of the Centervue Compass FAP are visible as an overlay on a red-free fundus image, with the orange/red test locations indicating reduced sensitivity. Note that the affected locations in the superior retina correspond to the location of the RNFL wedge defect (red outline), but there are additional locations of reduced sensitivity in the inferior retina as well (green outline). The Total Deviation (B) and Pattern Deviation (C) maps confirm that the VF loss corresponds to the location of the wedge defect in the superior retina.

Diagnostic Imaging

The patient was scanned with the SPECTRALIS SD-OCT imaging platform equipped with MultiColor and the Glaucoma Module Premium Edition (GMPE). The OD MultiColor image offers clear visualization of the RNFL wedge defect (Fig. 1). The circumpapillary RNFL thickness results derived from the 3.5 mm RNFL circle scan correspond with the narrow wedge defect seen on the MultiColor image. Since the wedge defect presents superiorly as it reaches the 3.5 mm circle scan, on the border of the temporal superior (TS) and nasal superior (NS) sectors, the results of the 6-sector Garway-Heath comparison to the reference database (RDB) are "Within Normal Limits" for all sectors. Upon closer inspection, the TS RNFL thickness sector results are actually in the 6th percentile of the RDB. This result suggests that only 6% of the eyes that were included in the RDB had thinner RNFL thickness values. These percentiles indicate that although these sectors are colored green, they are close to being flagged as "Borderline" (<5%) and warrant careful observation.

The RNFL wedge defect can be observed as a dip in the RNFL TSNIT plot, in the circumpapillary B-scan, and as "Borderline" in the superior quadrant of the ISNT analysis (Fig. 3, red arrows). The 4.1 mm and 4.7 mm RNFL circle scans confirm the presence and extent of this wedge defect (Fig. 4A, B, C). As the wedge defect extends away from the optic nerve head, it follows the arcuate pattern of the RNFL and presents itself in the TS sector results of the larger circle scans (Fig. 4B,C). A hole within the RNFL can be seen in the TS region of the 4.7 mm OCT B-scan (Fig. 4C), offering additional confidence in the associated SD-OCT results and allowing for the extent of the defect to be appreciated. The Bruch's Membrane Opening - Minimum Rim Width (BMO-MRW) measurements of the neuroretinal rim indicate "Borderline" thinning in the inferior sectors (Fig. 5). There is a dip in the NS sector that corresponds to the observed superior RNFL wedge defect.

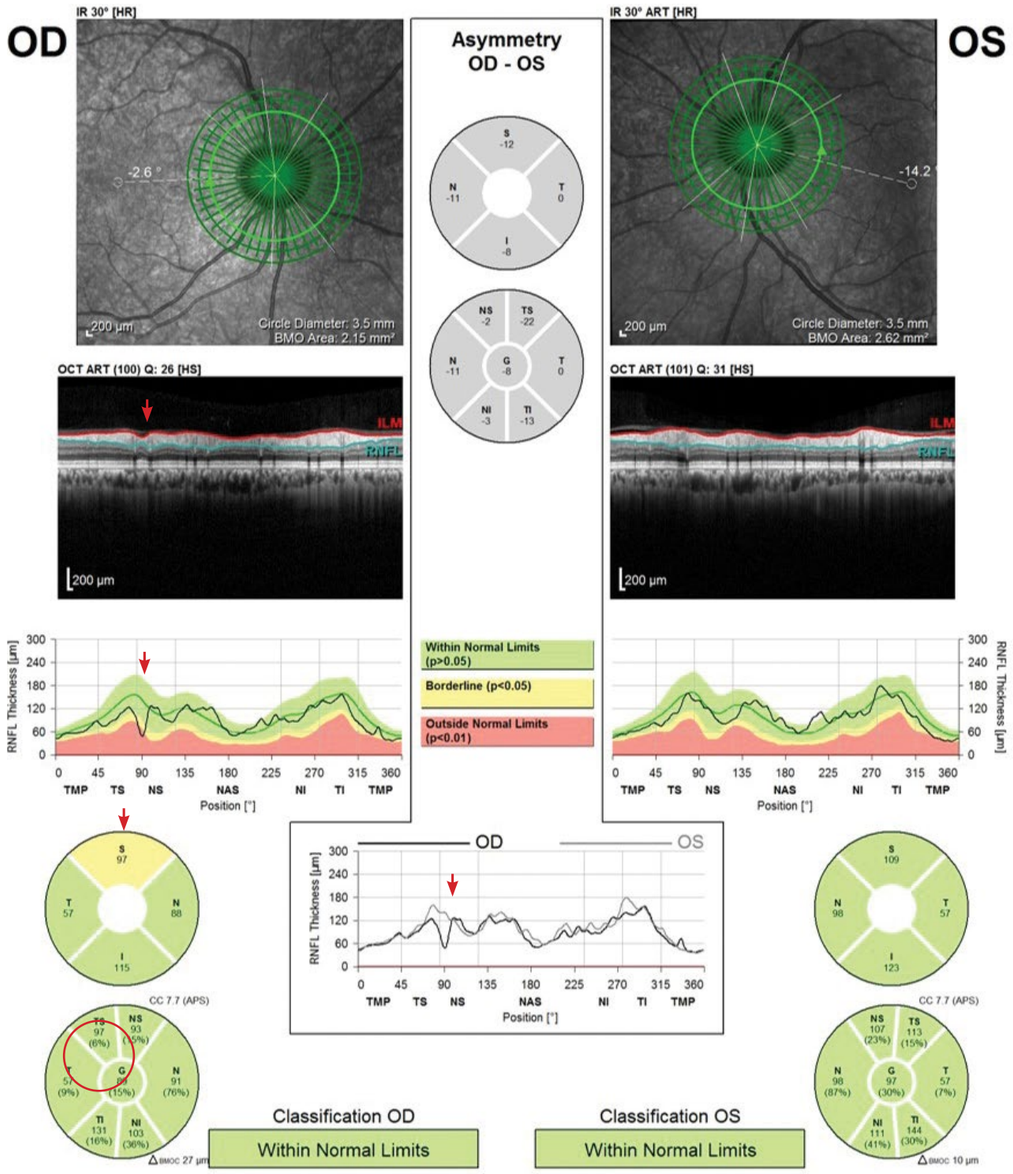

Figure 3. The GMPE RNFL Single Exam Report OU. The wedge defect can be visualized on the B-scan, the TSNIT profile, and the OD/OS comparison plot (red arrows). Note that the TS sector of the right eye shows RNFL thickness results in the 6th percentile, suggesting that this sector is close to being flagged as "Borderline" (red circle).

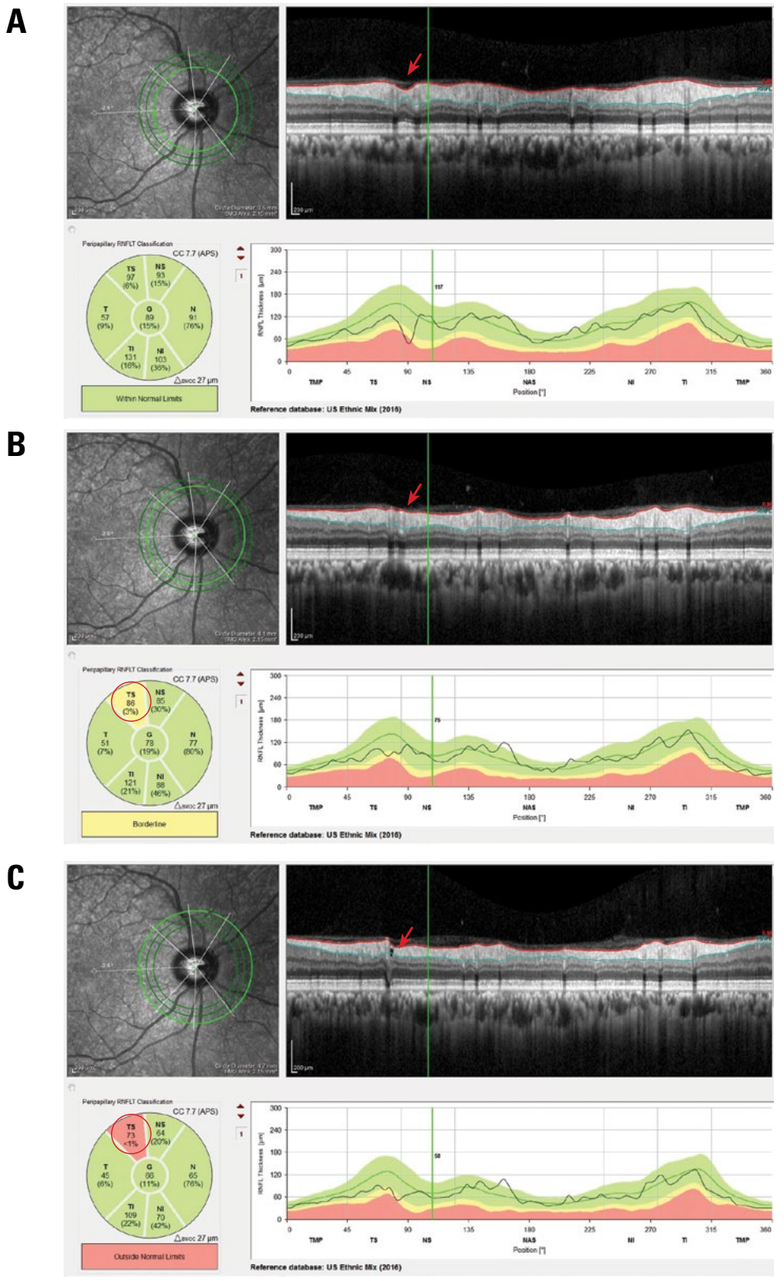

Figure 4. (A) The 3.5 mm GMPE RNFL circle scan shows "Within Normal Limits" circumpapillary RNFL thickness in all sectors, with the TS and NS sectors presenting with results in the 6th and 15th percentiles, respectively. The wedge defect can be visualized on the B-scan and the TSNIT profile (red arrows). (B) The 4.1 mm RNFL circle scan results indicate borderline thinning in the TS sector, confirming the wedge defect seen in the 3.5 mm scan (red circle). (C) The 4.7 mm RNFL scan results indicate "Outside Normal Limits" thinning in the TS sector (red circle). There is also an RNFL hole that can be seen in this B-scan, possibly related to RNFL thinning (red arrow).

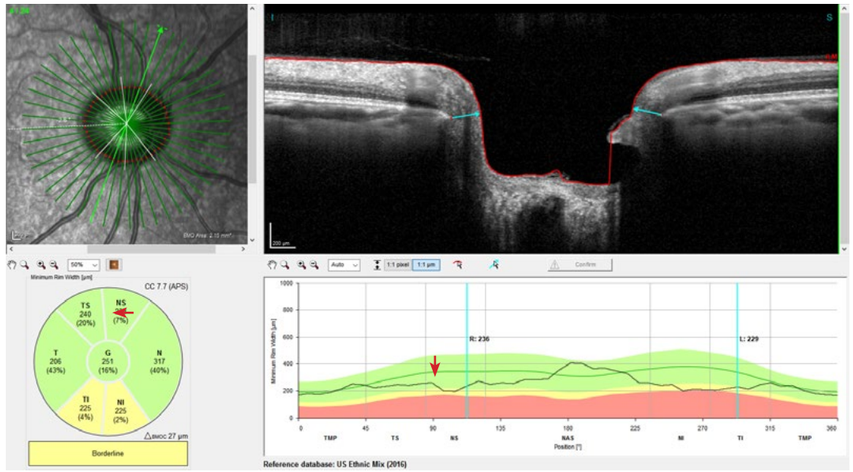

Figure 5. BMO-MRW analysis of the neuroretinal rim. For each of the 24 radial scans, BMO was automatically identified by the software and confirmed by the operator on the SD-OCT scans. The temporal inferior (TI) and nasal inferior (NI) sectors are flagged as "Borderline" when compared to the RDB. While the TS and NS sectors are noted as green, a dip in the TSNIT profile within the these sectors is indicative of damage (NS in the 7th percentile, red arrows).

Conclusion

This patient with POAG presents with a focal superior RNFL wedge defect OD. The examination findings are supported by both the SPECTRALIS GMPE scans and the perimetry results. The RNFL and neuroretinal rim (BMO-MRW) results confirm the findings on multiple levels, while the high-resolution B-scans further elucidate these numeric findings. The SPECTRALIS MultiColor imaging of the right eye illustrates the RNFL wedge defect, while the VF results show reduced threshold values that correspond in location to this defect (Fig. 2). These complementary findings enhance the diagnosis of glaucoma while confirming the need to monitor this patient carefully in order to mitigate possible progression of the disease.

Murray Fingeret, OD

Clinical Professor, State University of New York, College of Optometry, New York, NY, USA

Dr. Murray Fingeret, a graduate of the New England College of Optometry, completed a residency at the Joseph C. Wilson Health Center in Rochester, New York. He is Chief of the Optometry Section, Brooklyn/St. Albans Campus, Department of Veterans Administration New York Harbor Health Care System.

Dr. Fingeret sits on the Board of Directors of the Glaucoma Foundation and is a member of the American Glaucoma Society, the American Optometric Association, and the National Academies of Practice. He is a founding member and past president of the Optometric Glaucoma Society.

Case Presentation 3: Managing Asymmetric Glaucomatous Damage with SD-OCT, MultiColor Imaging, and Visual Fields, Donald C. Hood, PhD, and Robert Ritch, MD

A 62-year-old female presented with primary open-angle glaucoma (POAG). The clinical exam and optic disc photographs of the right eye (OD) of this patient were indicative of glaucoma, with optic disc cupping, a temporal inferior (TI) retinal nerve fiber layer (RNFL) wedge defect, and an inferior disc hemorrhage (Fig. 1). There is more advanced cupping in the left eye (OS), and this case will discuss both eyes (OU).

Standard Automated Perimetry (SAP) was performed on the Humphrey Field Analyzer (HFA) using the Swedish Interactive Thresholding Algorithm Standard (SITA-Standard) with the 24-2 and 10-2 test patterns. The SAP 24-2 visual field (VF) results of the right eye presented with a "Within Normal Limits" mean deviation (MD = -0.96 dB) and abnormal pattern standard deviation (PSD = 2.14 dB, P < 5%). The SAP 10-2 VF results agree with the 24-2 results, and indicate a cluster of abnormal test locations in the superior hemifield (MD = -0.67 dB; PSD = 1.72 dB, P < 5%). There is more extensive VF loss OS, and it has progressively worsened over time. The SAP 24-2 MD was -3.58 dB in 2009 and -13.18 dB in 2013. The SAP 10-2 MD was -8.96 dB in 2009 and -20.16 dB in 2013 (Fig. 3).

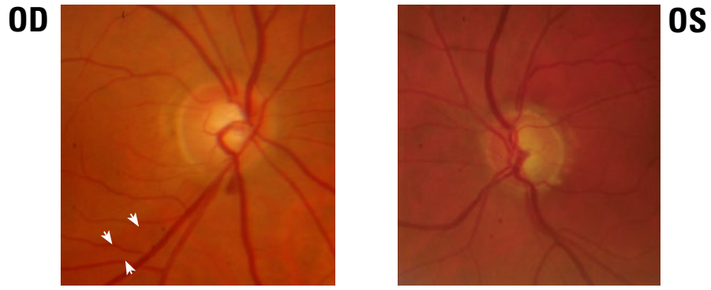

Figure 1. An optic disc photograph of the right eye shows a TI RNFL wedge defect that is difficult to visualize (white arrows) along with an inferior optic disc hemorrhage. There is advanced optic disc cupping OS, particularly in the superior and inferior regions.

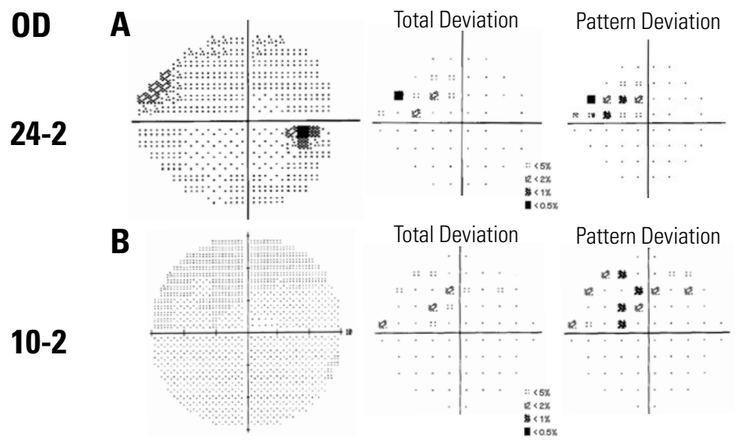

Figure 2. SAP results on the HFA using the SITA-Standard with the 24-2 and 10-2 test patterns are shown. (A) The VF results using the 24-2 test pattern show signs of sensitivity loss in the superior hemifield (MD = -0.96 dB, PSD = 2.14 dB, P < 5%). (B) The 10-2 test pattern results confirm the 24-2 results, with several test locations showing significant loss of sensitivity in the superior hemifield (MD = -0.67 dB; PSD = 1.72 dB, P < 5%).

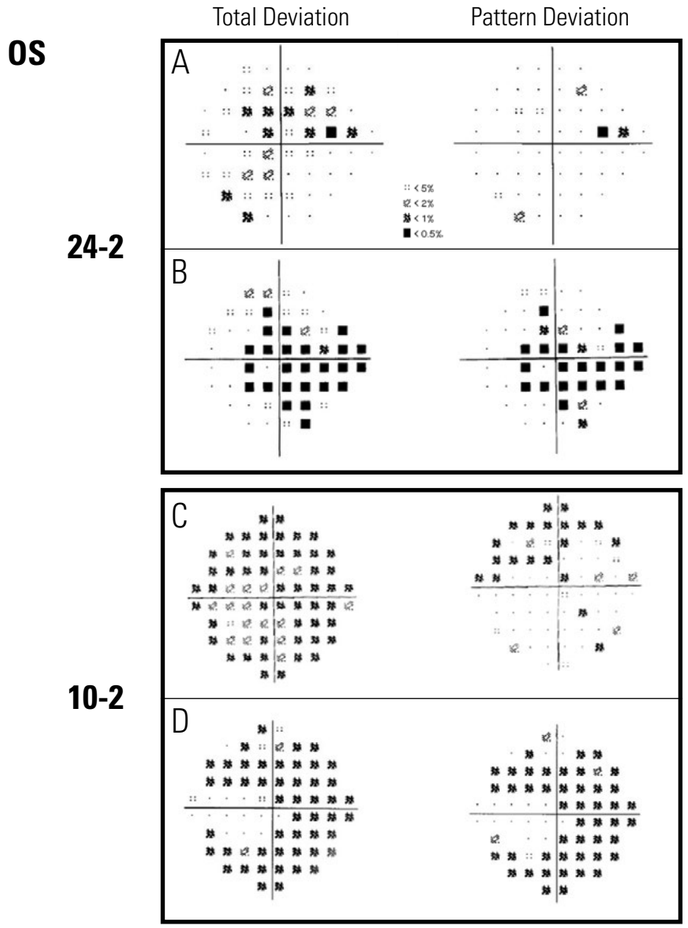

Figure 3. SAP testing of the left eye over a period of four years, assessed using the 24-2 and 10-2 SITA patterns. (A) The Total Deviation and Pattern Deviation are shown for 24-2 VF testing on June 11, 2009. There are significant deficits in all quadrants. (B) Four years later, the VF deficits have progressed. (C) For the 10-2 SITA pattern, VF testing shows similar deficits in the central 10 degrees. (D) There is similar progressive loss of sensitivity four and a half years later.

Diagnostic Imaging - Right Eye

The patient was imaged with the SPECTRALIS MultiColor and Glaucoma Module Premium Edition (GMPE) scans. The MultiColor (MC) image, composed of infrared (815 nm), green (515 nm), and blue (486 nm) wavelengths, offers a clear visual of the TI retinal nerve fiber layer (RNFL) wedge defect (Fig. 4). The GMPE scans of the circumpapillary RNFL confirm the TI wedge defect on the B-scan, the TSNIT profile, and the 6-sector Garway-Heath classification (Fig. 5). Also, the nasal inferior (NI) RNFL thickness is within the 13th percentile as compared with the reference database (RDB). The Bruch's Membrane Opening - Minimum Rim Width (BMO-MRW) results indicate neuroretinal rim thinning in the TI and NI sectors (Fig. 6). The NI disc hemorrhage seen on the optic disc photograph coincides with the NI BMO-MRW measurements. Finally, a scan of the posterior pole reveals ganglion cell layer (GCL) loss corresponding to the RNFL and BMO-MRW thinning (Fig. 7). All of these measurements are consistent with the VF results (Fig. 2).

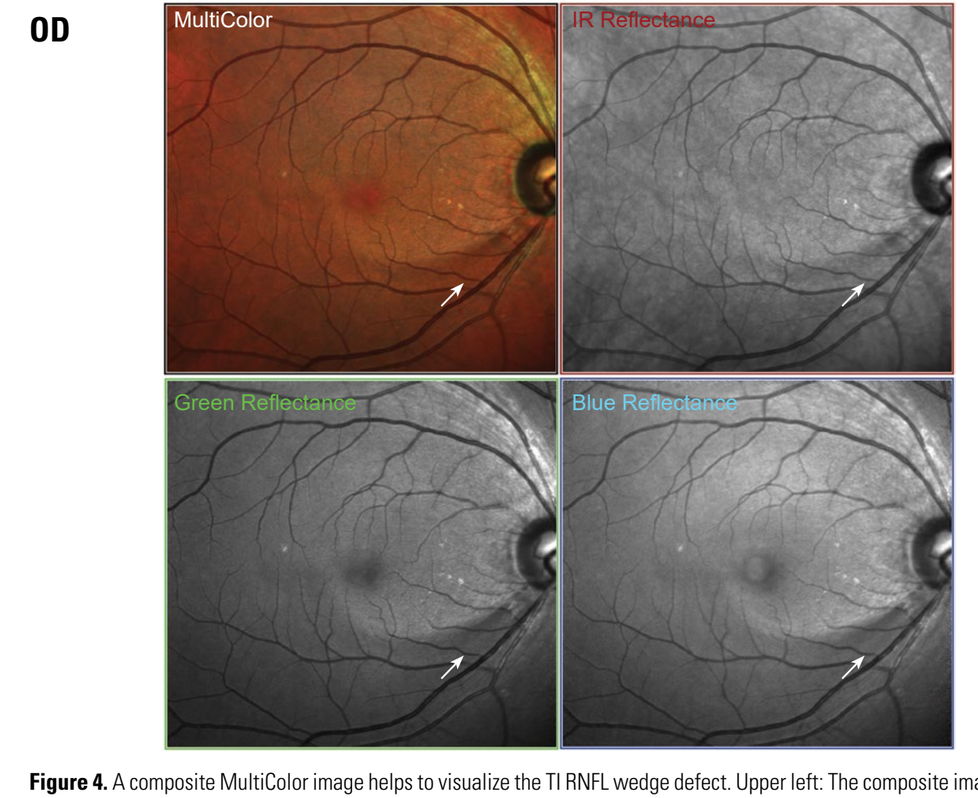

Figure 4. A composite MultiColor image helps to visualize the TI RNFL wedge defect. Upper left: The composite image is created from the combination of the IR (top right), green (bottom left), and blue (bottom right) reflectance images. While all images show the TI RNFL wedge defect, the extent and boundaries of the defect can be better appreciated on the blue and green reflectance images. Such images serve as confirmatory information to the other imaging modalities.

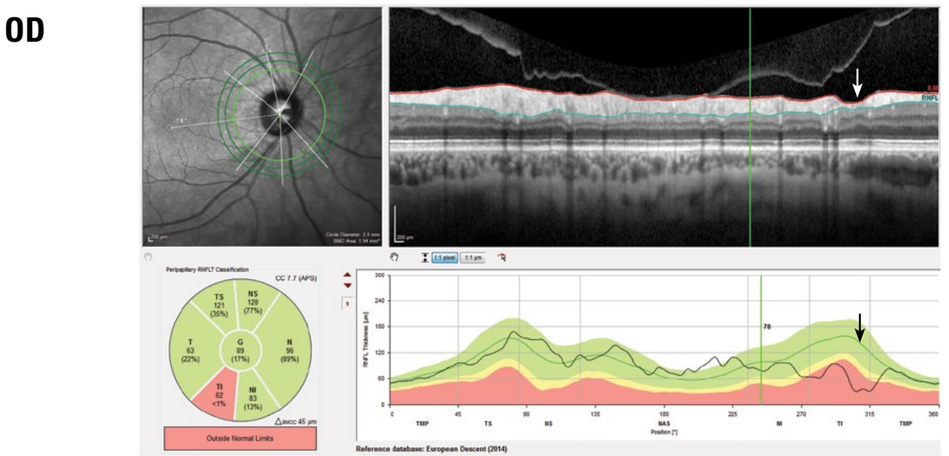

Figure 5. The GMPE RNFL scan 6-sector Garway-Heath results show that the circumpapillary RNFL is significantly thin in the TI sector. The RNFL wedge defect is also seen on the B-scan and the TSNIT profile (white and black arrows).

OD

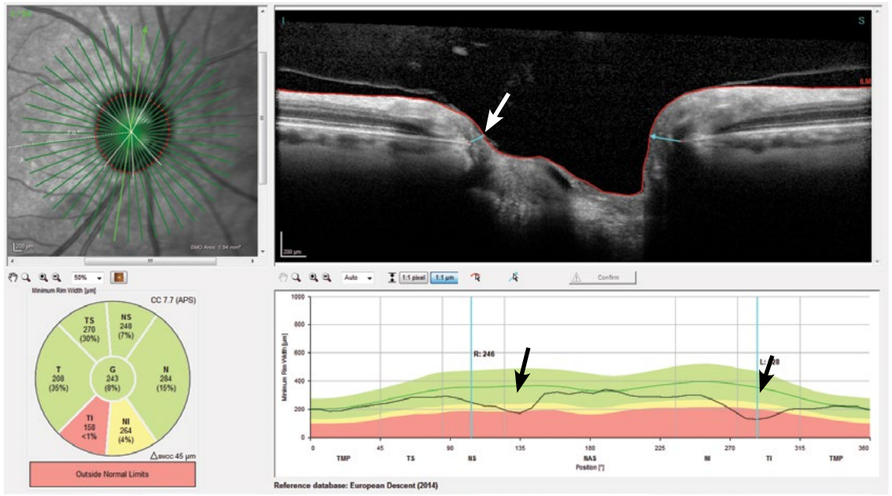

Figure 6. The BMO-MRW 6-sector Garway-Heath analysis and the TSNIT profile indicate neuroretinal rim thinning in the TI and NI sectors (black arrows), while the RNFL results indicate significant loss in only the TI sector. The inferior neuroretinal rim thinning can be confirmed on the B-scans (white arrow).

OD

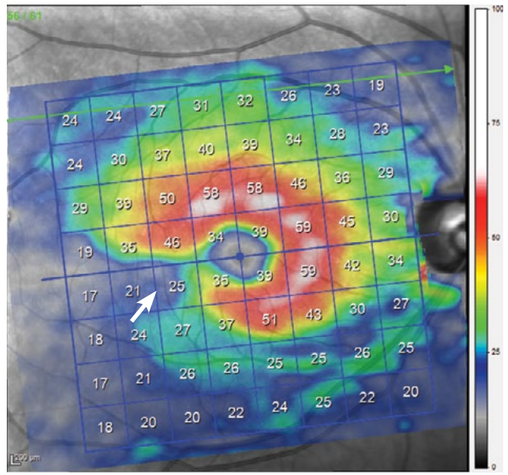

Figure 7. The GCL thickness color map shows ganglion cell loss that directly corresponds to the structural and functional findings (white arrow).

Diagnostic Imaging - Left Eye

The MultiColor image of the left eye indicates extensive RNFL loss (Fig. 8). The GMPE RNFL circle scan results also show significant defects in both the B-scan and the TSNIT thickness profile (Fig. 9). The BMO-MRW results show thinning of the neuroretinal rim in almost all sectors, with only the temporal sector being flagged as "Within Normal Limits" (9th percentile, Fig. 10). Finally, the posterior pole total retinal thickness and GCL thickness maps confirm the glaucomatous damage observed on the RNFL and BMO-MRW results (Fig. 11).

OS

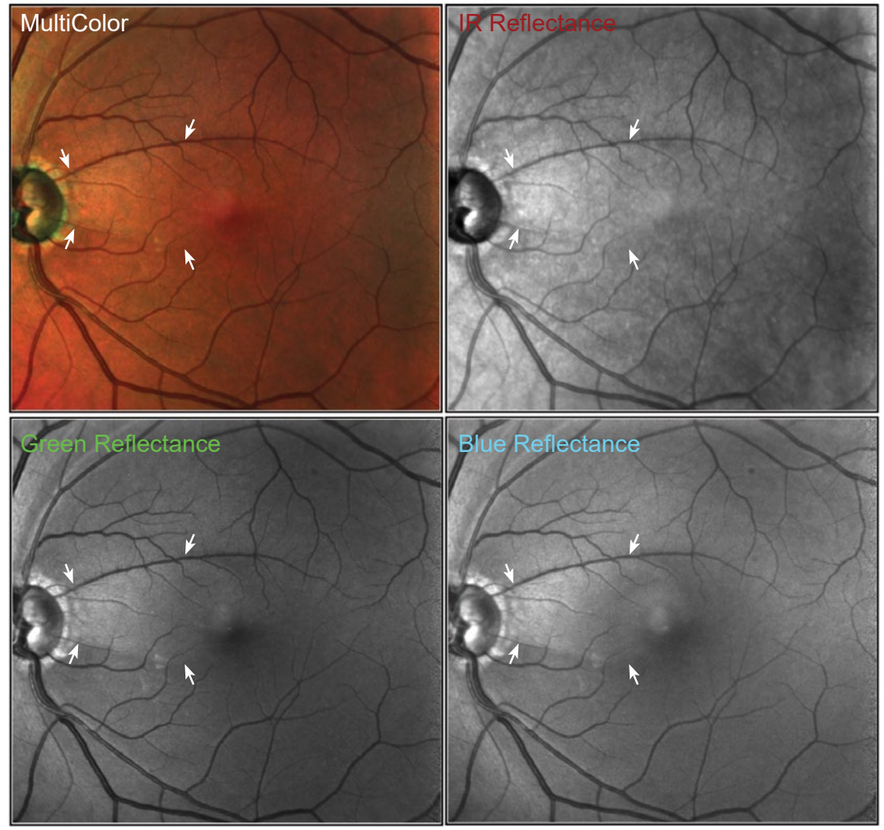

Figure 8. A composite MultiColor image helps to visualize the extent of the RNFL loss. The white arrows indicate the remaining RNFL in the MultiColor, IR, Green, and Blue reflectance images.

OS

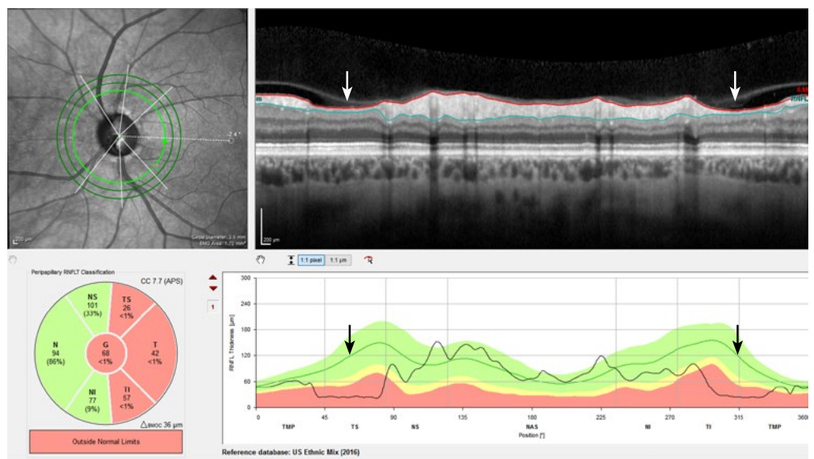

Figure 9. The GMPE RNFL circle scan 6-sector Garway-Heath analysis shows that the circumpapillary RNFL is significantly thin in all temporal sectors. The extent of the RNFL defects can be seen in the B-scan and the TSNIT profile (white and black arrows, respectively).

OS

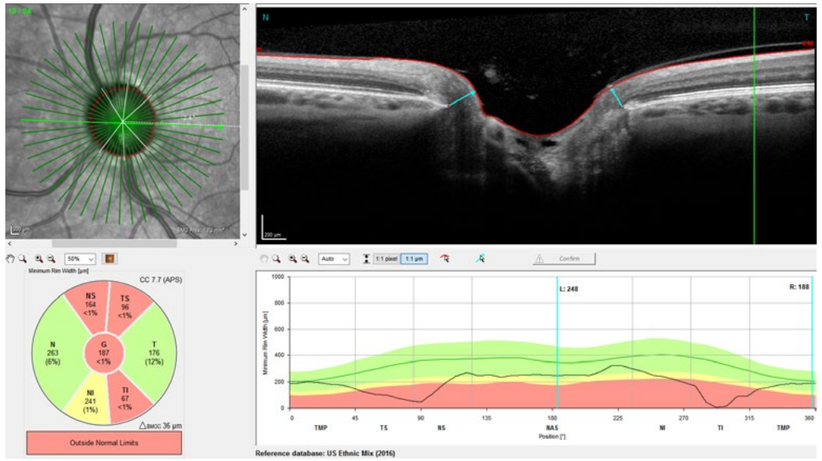

Figure 10. The BMO-MRW 6-sector Garway-Heath analysis indicates neuroretinal rim thinning in superior and inferior sectors, corresponding to the RNFL defects. The nasal and temporal sectors are also both relatively thin, indicating global neuroretinal rim thinning.

OS **A** **B**

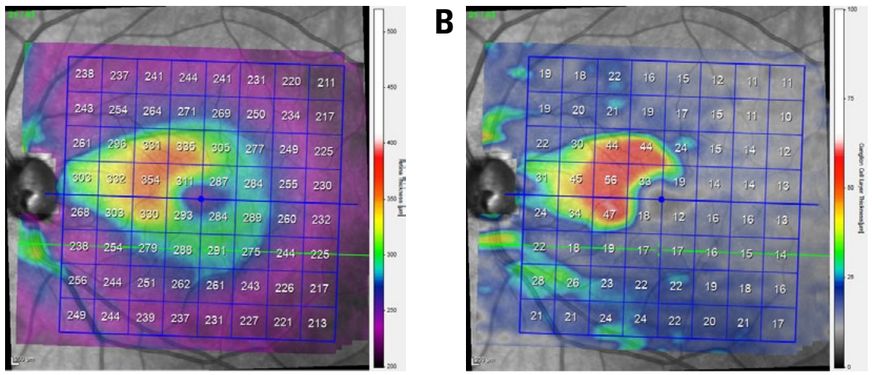

Figure 11. The total retinal thickness (A) and GCL thickness (B) color maps show ganglion cell loss that corresponds to the structural and functional findings.

Conclusion

Both eyes of this patient have functional and structural loss characteristic of glaucoma. The GMPE scans offer confirmatory diagnostic parameters and assist in the appreciation of the different disease stages of this patient's eyes. The MultiColor images illustrate the extent and boundaries of the RNFL wedge defects with more detail and clarity than the traditional fundus photos (Figs. 4 and 8). For the right eye, while the SAP 24-2 and 10-2 reports show signs of focal damage measured by PSD, their MD values are both "Within Normal Limits." However, the RNFL thickness, BMO-MRW, and GCL analyses confirm that there is significant structural damage that corresponds in location to the suspected location of the functional loss.

For the left eye, the VF results indicate rapid progression, and the GMPE scans will offer useful information for monitoring additional disease progression. In particular, while the VF and RNFL scans are close to their respective "floor" values, the BMO-MRW measurements and macular GCL thickness results may still measure further glaucomatous damage to the neuroretinal rim. Together, the GMPE scans and the VF results can help with careful monitoring of progressive changes, refining treatment decisions to preserve this patient's vision.

Donald C. Hood, PhD

Columbia University, New York, NY, USA

Donald C. Hood, the James F. Bender Professor of Psychology and Professor of Ophthalmic Science (in Ophthalmology), has been a member of the Columbia faculty since 1969. He holds MSc and PhD (1970) degrees from Brown University and honorary degrees from Smith College (2000) and Brown University (2017). He is an elected Fellow of the American Academy of Arts and Sciences and a recipient of an Alcon Research Institute Award (2014). He currently serves on the editorial boards of IOVS (since 1992), Translational Vision Science & Technology (since 2011), and Documenta Ophthalmologica (since 2004). He will be Editor-in-Chief of IOVS as of January 2018. While some of his 300 publications deal with issues of the basic neuroscience of vision, most of his work over the last 25 years has concerned research on diseases of the retina and optic nerve. He has had continuous grant support from NIH/NEI for 45 years.

Robert Ritch, MD

New York Eye and Ear Infirmary, New York, NY, USA

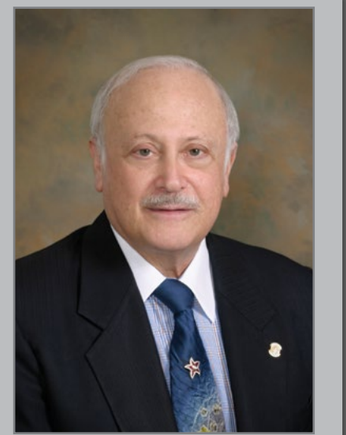

Dr. Robert Ritch holds the Shelley and Steven Einhorn Distinguished Chair in Ophthalmology and is Surgeon Director Emeritus and Chief of Glaucoma Services at the New York Eye & Ear Infirmary of Mount Sinai, New York City and Professor of Ophthalmology. He has devoted his career to broadening our understanding of the underlying etiologies and mechanisms of glaucoma and innovation in its medical, laser, and surgical treatment. When still a fellow in 1978, he performed the first laser iridotomy in New York and initiated the first course on laser treatment of glaucoma at the American Academy of Ophthalmology. He developed argon laser peripheral iridoplasty for the treatment of angle closure more complicated than pupillary block, which was instrumental in dealing with angle closure in East Asia, and taught on the diagnosis and treatment of angle closure around the world. His other major interests throughout his career have been pigment dispersion syndrome, exfoliation syndrome, and normal-tension glaucoma, to which he has made seminal contributions. He is a world leader in exfoliation syndrome, which affects 80 million people, and has started a global consortium to work on preventing, reversing, and even curing this disease.

Dr. Ritch has co-authored or edited nine textbooks and over 1800 medical and scientific papers, book chapters, articles and abstracts. He has presented over 750 lectures worldwide, including 50 named lectures and has received over 60 national and internatonal awards and medals.

HEIDELBERG ENGINEERING ACADEMY

Headquarters
Heidelberg Engineering GmbH · Max-Jarecki-Str. 8 · 69115 Heidelberg · Germany
Tel. +49 6221 64630 · Fax +49 6221 646362

AUS
Heidelberg Engineering Pty Ltd · 404 Albert St. · East Melbourne 3002 · Victoria
Tel. +61 396 392 125 · Fax +61 396 392 127

CH
Heidelberg Engineering GmbH · Schulstrasse 161 · 8105 Regensdorf
Tel. +41 44 8887 020 · Fax +41 44 8887 024

UK
Heidelberg Engineering Ltd. · 55 Marlowes · Hemel Hempstead · Hertfordshire HP1 1LE
Tel. +44 1442 502 330 · Fax +44 1442 242 386

USA
Heidelberg Engineering, Inc. · 10 Forge Parkway · Franklin, MA 02038
Tel. +1 508 530 7900 · Fax +1 508 530 7901

www.HeidelbergEngineering.com